


# Multiple Sources of Introduction of North American *Arabidopsis thaliana* from across Eurasia

Gautam Shirsekar,<sup>1</sup> Jane Devos,<sup>1</sup> Sergio M. Latorre,<sup>1,2</sup> Andreas Blaha,<sup>1</sup> Maique Queiroz Dias,<sup>†,1</sup> Alba González Hernando,<sup>1</sup> Derek S. Lundberg,<sup>1</sup> Hernán A. Burbano,<sup>1,2</sup> Charles B. Fenster,<sup>3</sup> and Detlef Weigel <sup>\*,1</sup>

<sup>1</sup>Max Planck Institute for Developmental Biology, Tübingen, Germany

<sup>2</sup>Centre for Life's Origin and Evolution, University College London, London, United Kingdom

<sup>3</sup>Oak Lake Field Station, Department of Natural Resource Management, South Dakota State University, Brookings, SD, USA

<sup>†</sup>Federal University of Viçosa, Viçosa, MG, Brazil

\*Corresponding author: E-mail: weigel@weigelworld.org.

Associate editor: Michael Purugganan

## Abstract

Large-scale movement of organisms across their habitable range, or migration, is an important evolutionary process that can shape genetic diversity and influence the adaptive spread of alleles. Although human migrations have been studied in great detail with modern and ancient genomes, recent anthropogenic influence on reducing the biogeographical constraints on the migration of nonnative species has presented opportunities in several study systems to ask the questions about how repeated introductions shape genetic diversity in the introduced range. We present an extensive overview of population structure of North American *Arabidopsis thaliana* by studying a set of 500 whole-genome sequenced and over 2,800 RAD-seq genotyped individuals in the context of global diversity represented by Afro-Eurasian genomes. We use methods based on haplotype and rare-allele sharing as well as phylogenetic modeling to identify likely sources of introductions of extant N. American *A. thaliana* from the native range in Africa and Eurasia. We find evidence of admixture among the introduced lineages having increased haplotype diversity and reduced mutational load. We also detect signals of selection in immune-system-related genes that may impart qualitative disease resistance to pathogens of bacterial and oomycete origin. We conclude that multiple introductions to a nonnative range can rapidly enhance the adaptive potential of a colonizing species by increasing haplotypic diversity through admixture. Our results lay the foundation for further investigations into the functional significance of admixture.

**Key words:** *Arabidopsis thaliana*, population genetics, admixture, nonnative species, migration.

## Introduction

*Arabidopsis thaliana* is predominantly a human commensal that is native to Africa and Eurasia. Its demographic history is filled with episodes of range expansions, bottlenecks, migrations, and admixture. Current models of *A. thaliana*'s population history highlight the recurrent theme of lineage migration and admixture with locally adapted genotypes in the native range of the species (Durvasula et al. 2017; Lee et al. 2017; Zou et al. 2017; Fulgione and Hancock 2018; Fulgione et al. 2018; Hsu et al. 2019). A further opportunity to learn about the impact of demographic processes and selection in *A. thaliana* arises from its relatively recent colonization of North America.

When a species is introduced outside its native range, where its long-term eco-evolutionary history has been established, different factors determine how well the introduced population adapts to the new environment. These factors include, but are not limited to history of introduction, founder effects, and strength of natural selection (Colautti and Lau 2015; Estoup et al. 2016). In the post-Columbian

era, *A. thaliana* has benefited from mostly unidirectional cross-continental species movement facilitated by human migrations to N. America (La Sorte et al. 2007; Winter et al. 2010). Thus, the N. American *A. thaliana* metapopulation presents a unique natural experiment for studying the role of history in explaining extant diversity and understanding how the colonizers have thrived despite population bottlenecks and seemingly low genetic diversity, also known as genetic paradox of invasion (Allendorf and Lundquist 2003). Important questions that can be addressed using this study system are: How much of the native diversity was introduced to N. America? How much new diversity has been generated in situ through mixing of lineages that originated from distant parts in the native range? How much of the observed diversity is due to selection?

*Arabidopsis thaliana* has become established across much of N. America. Coarse-scale population structure analysis of N. American individuals with 149 single-nucleotide polymorphism (SNP) markers has revealed the presence of a dominant lineage "Haplogroup1" (Hpg1) (Platt et al. 2010).

© The Author(s) 2021. Published by Oxford University Press on behalf of the Society for Molecular Biology and Evolution.

This is an Open Access article distributed under the terms of the Creative Commons Attribution License (<https://creativecommons.org/licenses/by/4.0/>), which permits unrestricted reuse, distribution, and reproduction in any medium, provided the original work is properly cited.

Open Access

Patterns of mutation accumulation in the genomes of pure Hpg1 individuals have supported an arrival in N. America about 400 years ago, soon after Europeans started to arrive en masse on the continent. A parsimonious explanation of the ubiquitous nature of this lineage could be that it was the earliest to be introduced to N. America (Exposito-Alonso, Becker, et al. 2018). So far, little consideration has been given to the supposedly subsequent arrival of other lineages, their origins in the native range, their fate as migrations continued during the past centuries, and how the genomes of the current N. American population have been shaped by processes such as admixture and adaptation.

We present the fine-scale population structure of the N. American *A. thaliana* population as viewed through the lens of range-wide genetic diversity of the species. Using genomes of *A. thaliana* individuals collected from the Midwest, the Eastern Seaboard, and the North–East of the current United States, we infer possible sources of ancestry based on haplotype-sharing, phylogenetic tree-based modeling, and rare allele sharing (RAS) with the worldwide data set. We also describe how admixture in this predominantly selfing species is generating new haplotype diversity and how admixture affects the fate of deleterious mutations and allows selection on immunity-related loci. The work presented here shows that increased global connectivity through the past two centuries has made species invasions from across the species range common and could have accelerated invasion of N. American habitat by avoiding the genetic paradox of invasion. Further, our work highlights that processes such as admixture and selection that determine success of lineages in the native range play a similarly important role in the non-native range.

## Results

### An Overview of Population Structure and Genetic Variation from RAD-Seq

We collected *A. thaliana* samples across an area of about 1,200 by 900 km in the Eastern United States during the spring seasons (mid-March to early June) of 2014, 2015, and 2016 (fig. 1 and supplementary table S1a and b, Supplementary Material online). We genotyped these samples using a RAD-seq implementation of reduced representation sequencing (Miller et al. 2007). After filtering for sequencing output and quality, we retained 2,861 individuals, which shared 4,907 polymorphic SNPs. In order to compare the population structure and genetic diversity in our N. American to the global Afro-Eurasian collection (AEA), we used data from the 1001 Genomes project (1001 Genomes Consortium 2016) in addition to whole-genome sequences (WGS) from 13 Irish (this work), ten African (Durvasula et al. 2017), and five Yangtze River basin accessions (Zou et al. 2017). From these AEA individuals, information on the 4,907 polymorphic SNPs found in our N. American individuals (average depth  $\sim 36\times$ ) were extracted and merged with the N. American data set for further analysis. Although pairwise similarity using “identity-by-state” (IBS) and “identity-by-descent” (IBD) across the genome is greater in N. American

than in AEA individuals, genetic variation relative to AEA individuals could nevertheless be observed in N. American individuals with principal component analysis (PCA) (supplementary fig. S1A, Supplementary Material online). North American individuals in our collection were genetically much more diverse than the N. American individuals previously sequenced as part of the 1001 Genomes Project (supplementary fig. S1B, Supplementary Material online).

### Diversity of N. American Haplogroups

We first used RAD-seq to rapidly genotype thousands of individuals, but because of its inherent biases (low density of markers, strand-bias, underestimation of genetic diversity), these data are not well suited for fine-scale, quantitative population genomic analyses (Arnold et al. 2013; Cariou et al. 2016; Lowry et al. 2017). We therefore selected and sequenced a subset of distantly related individuals with WGS approach, at an average of  $\sim 8\times$  coverage (0.63–43.91x, median=5.81x). A PCA of 500 N. American individuals, including a subset of previously analyzed herbarium individuals (Exposito-Alonso, Becker, et al. 2018) (supplementary fig. S1C, Supplementary Material online), resulted in an arrangement in which most individuals were found along distinct clines. We decided to explore this population structure in detail using different complementary population genetic methods.

Finer-scale population structure can be revealed by explicitly modeling the effects of linkage disequilibrium (LD) and clustering individuals based on their shared ancestry that emerges after accounting for LD (Busby et al. 2015; Leslie et al. 2015; Montinaro et al. 2015). Therefore, we hierarchically partitioned the N. American individuals into 58 clusters (from here on called *groups*) using a coancestry matrix derived using CHROMOPAINTER v2 and MCMC-based clustering in fineSTRUCTURE (Lawson et al. 2012) (supplementary fig. S3, Supplementary Material online). Haplogroup1 (Hpg1) is the most frequently observed *group* across the sampled populations (fig. 2), consistent with previous observations (Platt et al. 2010; Exposito-Alonso, Becker, et al. 2018). OHML (Ohio) and NJSC (New Jersey) had the highest within-population haplotype diversity, with 11 and 12 *groups*. Several *groups*, such as OhioNewJersey2, IndianaNewJersey1, and NewJerMich1, were found in populations from geographically distinct regions (fig. 2).

We further analyzed the genetic relationships among these *groups* using several complementary approaches. Treemix (Pickrell and Pritchard 2012), without considering migration edges, reconstructed relationships among the *groups* (supplementary fig. S4A, Supplementary Material online), similar to the topology inferred by fineSTRUCTURE clustering (supplementary fig. S3B, Supplementary Material online). Notably, residuals from the fitted model with high positive values indicated that the fit could be improved by including admixture edges among the *groups* (supplementary fig. S4B, Supplementary Material online). High positive residual values between Hpg1, which is the omni-present *group* with high frequency and other *groups*, suggested possible gene flow between them.

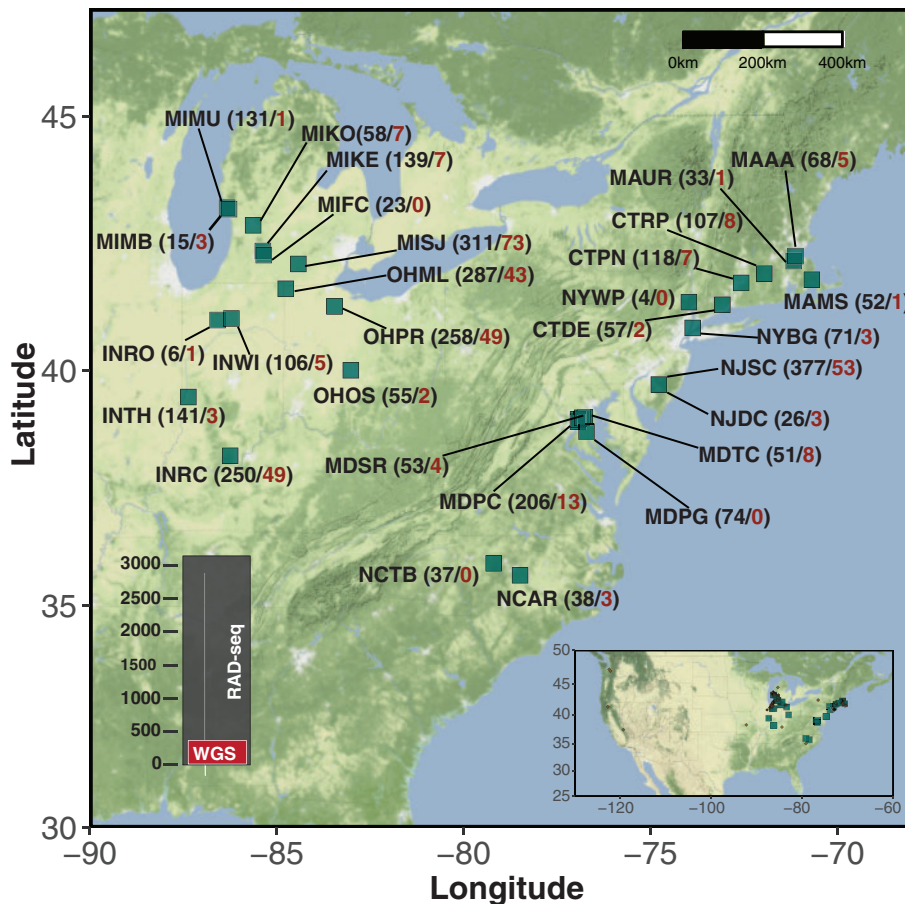


**Fig. 1.** Locations and number of sampled individuals. Abbreviations of the locations sampled are shown along with the number of RAD-sequenced samples (in black) and the number of whole-genome sequenced (WGS) samples (in red). Left inset: bar plot of total number of samples sequenced. Right inset: sampling area in the context of N. America.

Stochastic changes in allele frequency, as a result of the neutral process of drift, hold information about shared ancestry. We therefore estimated values for the  $f_3$ -outgroup statistic (Raghavan et al. 2014) to understand the shared drift among groups relative to an outgroup (individuals of relict ancestry). Relicts comprise highly diverged individuals from ice age refugia (Lee et al. 2017) and therefore were chosen as an outgroup. Indeed, some of the N. American groups (OhioMich1, SouthIndiana4, and Ohio7) along with Hpg1 shared excess drift with other groups (supplementary fig. S5, Supplementary Material online). As the  $f_3$ -outgroup test identifies the closest relative population and does not itself point to the admixture, we applied  $f_3$  statistic to explore the possibility of admixture among these groups (Patterson et al. 2012). We calculated values for the  $f_3$  statistic in all trios (*groupA*, *groupB*: *groupTest*) of N. American groups to detect whether *groupTest* was admixed between *groupA* and *groupB*. There were several *groupTest* examples with negative  $f_3$  scores and Z scores below  $-3$  in several trios (supplementary fig. S6A and table S2, Supplementary Material online). In several cases, Hpg1 emerged as a putative source (as either *groupA* or *groupB*) (supplementary table S2, Supplementary Material online). To investigate this in more detail, we calculated the shared drift of Hpg1 relative to the other N. American groups. We found more groups with a gradient of shared drift with

Hpg1; Massachusetts1 was one of the groups with least shared drift (supplementary fig. S6B, Supplementary Material online). Therefore, we calculated the ABBA-BABA statistic ( $D$ -statistic) in the form of (*Massachusetts1*, *Test: Haplogroup1*, *Relicts*) to learn the extent of gene flow between Hpg1 and other N. American groups (supplementary fig. S6C, Supplementary Material online). Many groups showed significantly more ABBA sites (Z score  $< -3$ ) than BABA sites, confirming the contribution of Hpg1 ancestry to the genetic makeup of these groups.

### Contribution of Distinct Sources of Ancestry to N. American Diversity

North American groups vary in terms of their drift relative to the earliest arrival, Hpg1, which suggests that there have been multiple introductions of *A. thaliana* to N. America. It is also unclear whether the observed haplogroups already existed in Eurasia, or whether they only formed by intercrossing in N. America. We therefore wanted to learn whether N. American extant haplogroups include ancestry from different geographic regions in Eurasia. We first excluded lineages that showed evidence of recent admixture (groups

with significantly negative  $f_3$ -scores), and we then applied statistical procedures based on shared haplotype chunks (fineSTRUCTURE), shared drift ( $f_3$ -outgroup,  $D$ -statistic, and

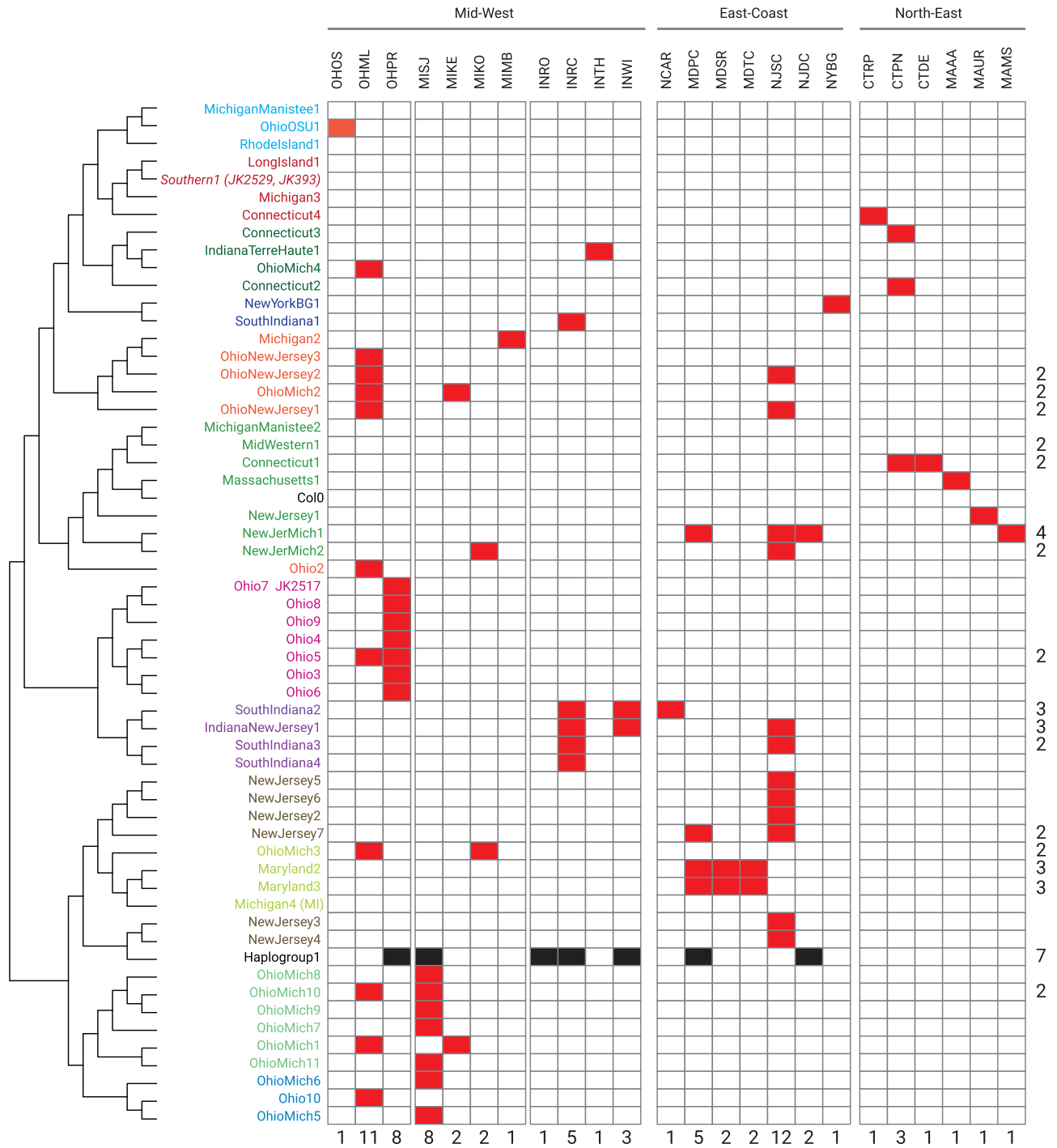


**Fig. 2.** Identification of North American groups based on haplotype sharing and their distribution in different populations. Collapsed fineSTRUCTURE tree generated by merging North American individuals into groups (herbarium individuals are denoted by JKxxx) based on their coancestry (derived using CHROMOPAINTERv2, coancestry matrix in [supplementary fig. S3, Supplementary Material](#) online). Last row of numbers represents the total count of groups present in the population, and last column of numbers represents the number of populations in which a specific group is present (here a group present in a single population is not counted, count=1).

qpWave) and enrichment of rare alleles with respect to the AEA haplotype diversity to identify sources of ancestry in Eurasia based on WGS from AEA individuals ( $n = 928$ ) (1001 Genomes Consortium 2016). We traversed the genomes of N. American individuals to assign local ancestry along each chromosome. To this end, we performed haplotype-based inference in three steps: 1) Paint each AEA

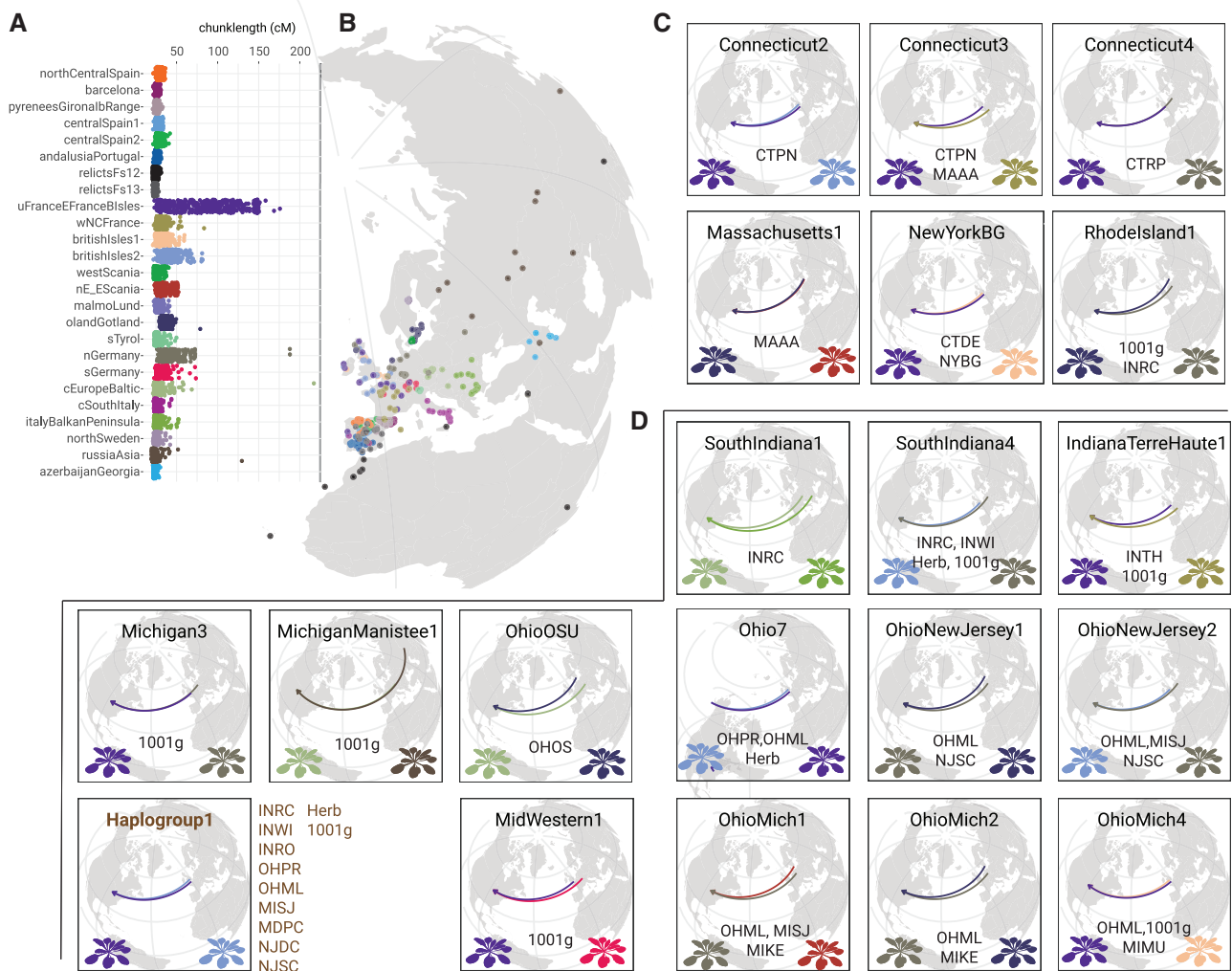
individual against the others (excluding itself) with CHROMOPAINTER v2, 2) Based on haplotype sharing, cluster individuals into subclusters using fineSTRUCTURE. These subclusters were then grouped into clusters, and clusters were further grouped into regions (supplementary fig. S7, Supplementary Material online; details of these hierarchical partitions for each AEA individual are given in supplementary

table S3, Supplementary Material online). 3) We chose 15 representative individuals per AEA region and estimated an ancestry profile for individual N. American recipients.

Figure 3A shows these inferred ancestry profiles for the N. American individuals. It can be seen that although the majority of groups are enriched for Upper/EastFranceBritishIsles ancestry, other British Isles regions (BritishIsles1 and BritishIsles2) also feature significantly across several groups (fig. 3C and D; supplementary fig. S8, Supplementary Material online). Apart from these, some N. American groups such as MichiganManistee1, OhioOSU, and SouthIndiana1 had substantially higher contributions from East European regions such as RussiaAsia, CentralEurope/Baltic, and Italy/BalkanPeninsula. NorthGermany and SouthGermany regions have contributed to the ancestry of OhioMich1, Rhodelsland1, and Mid-Western1 groups (fig. 3C and D; supplementary fig. S8, Supplementary Material online). These results also highlight how geo-genetically distant AEA

ancestries could be found within the same population (INRC) or within the same regions (Midwest) in N. America.

We explored these haplotype-sharing patterns further by measuring shared drift between a test N. American group and 158 subclusters of AEA individuals using  $f_3$ -outgroup statistic of the form  $test, subcluster; relictsFs12-3$  (We chose relictsFs12-3 as an outgroup as it is a highly diverged subcluster comprising relict population individuals) and building a maximum likelihood (ML) tree by fitting Treemix (Pickrell and Pritchard 2012) model without any admixture edges. At a coarser scale, the results agree with the haplotype-based inferences. Shared allelic drift measured with  $f_3$ -outgroup statistic and captured in the ML tree showed that the current N. American groups are related to the AEA subclusters that belonged to either western, central, or eastern Europe (supplementary figs. S9 and S10, Supplementary Material online). We also observed these patterns of relatedness qualitatively in a PCA plot where we projected N.



**FIG. 3.** Chromosome painting of N. American groups with Afro-Eurasian (AEA) regions as donors. (A) Copying profile of the N. American individuals inferred with CHROMOPAINTERv2 using a reference panel of individual haplotypes belonging to different AEA regions, each dot represents an individual (cumulative genomic segment length copied is in centiMorgans). (B) Geographic locations of the AEA individuals used in the reference panel (colored by region). (C, D) Two major contributions from AEA regions to N. American groups found on Eastern Seaboard-Northeast and Midwest. Arrows point from the mean geographic position of the AEA regions to that of the N. American groups (colors of the contributing region are the same as in panel [A]). Credit for original design of *A. thaliana* rosettes: Frédéric Bouché.

American individuals into PC space occupied by AEA individuals (supplementary fig. S11A, Supplementary Material online). Even finer details became apparent with uniform manifold approximation and projection (UMAP) embeddings (McInnes et al. 2018) (supplementary fig. S11B, Supplementary Material online) derived from the first 50 PC components of all the individuals (without projection).

The coarse patterns of shared ancestry emerging from  $f_3$ -outgroup statistic, PCA projection, and UMAP embeddings were tested in a more systematic way by evaluating the “treeness” of different topological configurations. We first calculated  $D$ -statistic (Green et al. 2010) for all the N. American nonadmixed groups (X) in the form of NorthGermany, RelictsFs12; X, *A. lyrata* (*Arabidopsis lyrata* as a closest relative to *A. thaliana*; Schmickl et al. 2010; was chosen as an outgroup). NorthGermany region was chosen because of its central geographic location among the possible sources of N. American *A. thaliana*. We then calculated  $D$ -statistics for the N. American groups by replacing NorthGermany with four regions: BritishIsles1, Upper/EastFranceBritishIsles, CentralEurope/Baltic, and RussiaAsia. We then plotted  $D$ -statistics with replacement regions to  $D$ -statistics obtained using NorthGermany separately to understand region specific drift (Ebenesersdóttir et al. 2018). These biplots (fig. 4C) clearly differentiate western and eastern European sources of ancestry in N. American *A. thaliana*. OhioOSU, Ohio2, SouthIndiana1, and MichiganManistee1 clearly showed the relative eastern European ancestry component. The analysis also revealed that Col-0, the reference genome accession for *A. thaliana* research, shares significant ancestry with individuals from NorthGermany, confirming the origin of Col-0 in or near Germany (Rédei 1992). Despite constrained “tree” topologies explored, since we used *subclusters* to estimate the  $D$ -statistic, it allowed us to capture variation in the shared drift (horizontal and vertical bars in fig. 4) experienced by a target N. American group with a given AEA region.

We extended this analysis using qpWave (Reich et al. 2012) to test whether any two N. American groups would be symmetrically related to a set of outgroups (AEA regions).

Specifically, we tested whether a set of  $f_4$ -statistics comprising two N. American groups across a set of layer1 outgroups (AzerbaijanGeorgia, Barcelona, NorthSweden, NorthWestEngland, Relicts Fs13, SouthTyrol, WestScania, and West/NorthCentralFrance) makes a matrix of rank 0 (same wave of ancestry) (supplementary table S4, Supplementary Material online). We then tested whether addition of an extra outgroup region (consisting of putative sources of ancestry) to the layer 1 outgroup set affected the symmetry of shared ancestry. If the two test N. American groups are differentially related to the extra outgroup region, then it would increase the rank of the original matrix of  $f_4$ -statistics (rejection of rank 0), indicating distinct streams of the ancestry among the test groups. We added an extra outgroup from additional regions of BritishIsles2, ItalyBalkanPeninsula, NorthGermany, RussiaAsia, and Upper/EastFranceBritishIsles one-by-one. Adding these putative source regions affected the symmetrical relationships observed with our original outgroup set. Except in the case of SouthIndiana4 and Ohio7, all the N. American group combinations showed asymmetric relationships (rejection of rank 0) with these extra outgroups (supplementary table S4, Supplementary Material online). These results validated the findings from qualitative observations made with PCA projection, and UMAP embeddings. It further confirmed results obtained from  $f_3$ -outgroup statistic, ML tree, and  $D$ -statistics analysis, that the N. American *A. thaliana* groups have ancestral components from western Europe (mainly British Isles), central Europe, and eastern Europe.

More subtle patterns of ancestry can be inferred by finding rare variants (Schiffels et al. 2016) from AEA that have risen to higher frequency in N. American individuals. Because we had moderate- to high-coverage whole genomes of the AEA and N. American individuals, we could use such rare variants to independently ascertain the results obtained from the haplotype-based ancestry inference and shared ancestry-based inference, mostly on moderate to high frequency alleles. We identified variants from AEA individuals with frequency of 1% or lower and tracked their enrichment in the N.

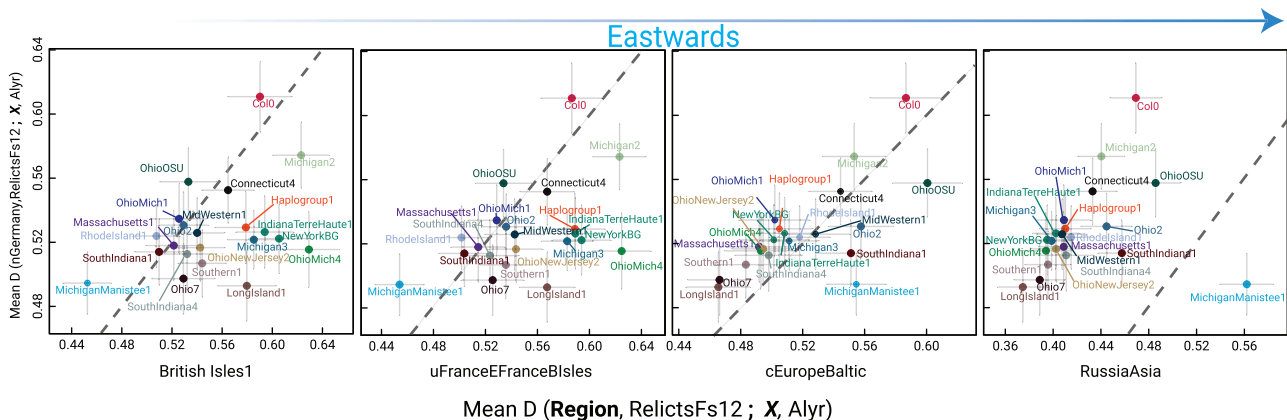


**FIG. 4.** Multiple sources of origin of N. American haplogroups. Biplot of mean  $D$ -statistics of N. American haplogroups (X) with *subclusters* comprising NorthGermany region (NorthGermany, RelictsFs12; X, *A. lyrata*), against mean  $D$ -statistics of *subclusters* comprising different regions in an eastward direction (testRegion, RelictsFs12; X, *A. lyrata*). Vertical and horizontal bars represent the spread of  $D$ -statistics from member *subclusters* of each region.

American groups. We found that N. American groups have accumulated rare alleles from different AEA subclusters (supplementary fig. S12, Supplementary Material online). Whereas several N. American groups have inherited rare alleles from British Isles subclusters, groups Rhodelsland1, MichiganManistee1, OhioOSU, SouthIndiana1, and OhioMich1 have accumulated rare alleles from central/eastern European subclusters, whereas Hpg1 has accumulated a significant number of rare alleles from subclusters from the Upper/EastFrance/BritishIsles region. Taken together, this analysis confirmed that N. America was colonized by *A. thaliana* in multiple waves with distinct sources of ancestry.

### Environmental Conditions at Source and Success of Colonizing Lineages

As we had inferred the shared ancestry of the colonizing lineages with different complementary methods, we hypothesized that besides human-assisted migration, environmental similarity between putative source subclusters and colonizing lineages contributed to successful colonization of the lineages. To test this hypothesis, we fit a regression model to predict shared ancestry with AEA subclusters (as measured by  $f_3$ -outgroup statistics of the form test N. American group, AEA subcluster: RelictsFs12\_3 (outgroup), value of the statistic is proportional to the shared ancestry between the populations relative to the outgroup), using linear combinations of four environmental variables: average temperature (avg), precipitation (prec), solar radiation (srad), and water vapor pressure (vapr). *Arabidopsis thaliana* shows significant local adaptation to climate (Exposito-Alonso, Vasseur, et al. 2018; Fulgione and Hancock 2018), thus the choice of these four variables should provide a general climatic niche. We used Bayesian multilevel modeling (bMLM) framework (Gelman 2006) to understand each N. American group's environmental association with its putative source AEA subclusters without ignoring the environmental association to the entire cohort of N. American groups.

Population-scale coefficients for the environmental variables precipitation (mm) and water vapor pressure (kPa) revealed that environmental dissimilarity calculated by Euclidean distance between each N. American group and AEA subcluster is negatively correlated with the  $f_3$ -outgroup statistics (table 1). Although average temperature dissimilarity is slightly negatively correlated with  $f_3$ -outgroup statistics, the compatibility interval with the model is large, with slightly positive correlation in posterior distribution. Upon closer examination of the coefficients estimated for individual N. American groups, it can be seen that precipitation and water vapor pressure dissimilarity is negatively correlated with the  $f_3$ -outgroup statistic for all groups but MichiganManistee1 (supplementary fig. S13, Supplementary Material online). Overall the general trend of negative correlation of the linear combination of the dissimilarity of the variables (average temperature, precipitation, solar radiation, and vapor pressure) to the  $f_3$ -outgroup statistic can be captured with the individual estimates sampled from the posterior distribution (supplementary fig. S14, Supplementary Material online).

**Table 1.** Posterior Summary of the Regression Coefficients for Environmental Variables.

Parameter	Mean	SD	hdi_3%	hdi_97%	$\hat{R}$
$\bar{a}$	0.1390	0.0920	-0.0280	0.3190	1.0000
$\beta_{T_{avg}}$	-0.0640	0.0960	-0.2420	0.1170	1.0000
$\beta_{prec}$	-0.1800	0.0910	-0.3530	-0.0080	1.0000
$\beta_{srad}$	-0.0010	0.0910	-0.1800	-0.1600	1.0000
$\beta_{vapr}$	-0.2320	0.0960	-0.4080	-0.0490	1.0000
$\sigma$	0.3950	0.0110	0.3730	0.4160	1.0000

NOTE.—Bayesian multilevel model-based pooled estimates of regression coefficients for environmental variables  $T_{avg}$  ( $^{\circ}\text{C}$ ), precipitation (mm), solar radiation ( $\text{kJ m}^{-2} \text{day}^{-1}$ ), and water vapor pressure (kPa).  $f_3$ -outgroup statistic of each N. American group to every AEA subcluster (outgroup: relicts Fs12\_3) was used as a Student's  $t$ -distributed dependent variable.

The negative correlation between environmental dissimilarity and shared ancestry led us to hypothesize that in reduced dimensional space of environmental variables (average temperature, precipitation, and vapor pressure), N. American groups should be closer to their source AEA subclusters. To test this, we performed UMAP on the standardized values for environmental variables for N. American groups and AEA clusters together, followed by hierarchical clustering on the reduced environmental space (see details in the Supplementary Material online). We observed that the N. American groups and their putative source clusters, as inferred by population genomic approaches (specifically subclusters from Upper/EastFranceBritishIsles, NorthGermany, SouthGermany, BritishIsles1, BritishIsles2, and CentralEurope/Baltic regions) occupied similar space in the UMAP embeddings (supplementary fig. S16, Supplementary Material online) and were in the same major clades (supplementary fig. S17, Supplementary Material online), thus confirming that overall environmental similarity between source populations and N. America might be an important contributor to the success of colonization.

### Effect of Admixture on Deleterious Mutations

Evolutionary theory predicts that during range expansions and new colonizations deleterious mutations accumulate gradually and steadily, resulting in increased mutational load that can be reduced again by outcrossing (Peischl et al. 2013). We hypothesized that the levels of mutational load in N. American individuals would be related to rates of historic outcrossing as inferred from admixture. To test this, we chose individuals from populations INRC, MISJ, NJSC, and OHPR because of: 1) Presence of earliest colonizing lineage Hpg1 and 2) two-way admixture events between Hpg1 and non-Hpg1 groups (supplementary fig. S6 and table S2, Supplementary Material online) in these populations. First, we inferred admixture proportion in the admixed groups by averaging local ancestry inference (LAI) obtained with Loter (Dias-Alves et al. 2018). We divided derived mutations observed in N. American groups into three different categories according to SIFT4G (Kumar et al. 2009) predictions (see details in Materials and Methods) and calculated the frequency of these mutations in each group including the source groups (Hpg1 and non-Hpg1s). Derived alleles with frequency

of 1 were considered as fixed, and based on the count we calculated fixed-to-total derived alleles ratios ( $\phi$ ) for each *group*. Considering admixture tracts of the diverged source lineages will result in slightly increased effective population sizes of the admixed groups, admixture is expected to reduce estimates of  $\phi$  regardless of mutational categories. As genome-wide synonymous derived variation is expected to be effectively neutral with respect to fitness in small populations (Walsh and Lynch 2018), we considered  $\phi_{\text{syn}}$  as a baseline for the reduction in  $\phi$  due to admixture and divergence, and therefore scaled  $\phi_{\text{non-syn-deleterious}}$  and  $\phi_{\text{non-syn-tolerated}}$  with  $\phi_{\text{syn}}$  (details in Materials and Methods). The scaled  $\phi_{\text{non-syn-deleterious}}$  ( $\Phi$ ) is significantly lower (Welch's *t*-test *P* value = 6.35e-12) than for nonsynonymous tolerated mutations (fig. 5 and supplementary fig. S18C and table S17, Supplementary Material online). Further, admixture had a strong effect on reducing  $\Phi_{\text{non-syn-deleterious}}$ , whereas  $\Phi_{\text{non-syn-tolerated}}$  was not affected by it (supplementary fig. S18B, Supplementary Material online). The change from,  $\Phi_{\text{non-syn-tolerated}}$  to  $\Phi_{\text{non-syn-deleterious}}$  was significantly different between admixed and source *groups* (supplementary fig. S18D, Supplementary Material online). Similar patterns were observed when  $\Phi$  was estimated using the total genome-wide  $\phi$  for scaling across mutational categories (supplementary fig. S18E, Supplementary Material online). This strongly suggests that admixture helps to eliminate derived mutations with potential deleterious impacts and it efficiently reduces nonsynonymous mutational load.

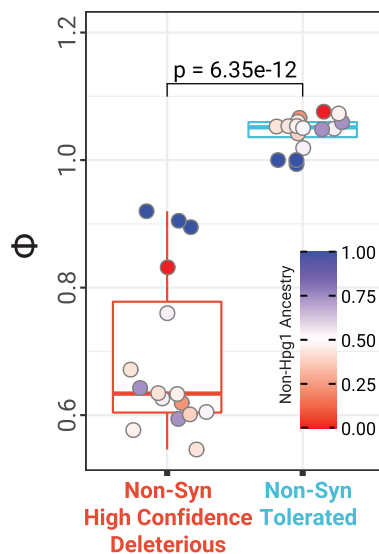


**Fig. 5.** Scaled fixed-to-total derived alleles ratios ( $\Phi$ ) for N. American *groups* across nonsynonymous mutation categories. Scaled fixed-to-total derived alleles ratio ( $\Phi$ ) for each *group* in populations OHPR, INRC, MISJ, and NJSC for nonsynonymous mutation categories was calculated, scaled by the fixed-to-total derived alleles ratio for synonymous mutations. Points represent different *groups* in the focal populations and colors of the individual points represent its non-Hpg1 ancestry proportion, as indicated on the scale at the right. Fixed derived alleles are alleles with frequency=1. *P* value is from Welch's *t*-test.

## Ongoing Selection at Several Immunity Loci in N. America

Apart from admixture potentially reducing mutational load, it can also be a source of beneficial alleles. If such alleles are strongly selected, they will create signatures of a selective sweep (Smith and Haigh 1974; Stephan 2019; Moest et al. 2020). To look for such a scenario, we focused on large populations comprising several *groups* that apparently arose as a result of admixture between lineages that diverged before their introduction to N. America (supplementary fig. S3, Supplementary Material online). These populations were INRC (Indiana), NJSC (New Jersey), MISJ (Michigan), OHML, and OHPR (both Ohio).

Methods that track the decay of haplotype homozygosity in a population (Vatsiou et al. 2016) can be used to detect such sweeps. We scanned whole genomes for signals of natural selection using haplotype homozygosity-based tests *iHS* (integrated haplotype homozygosity score) (Voight et al. 2006) and  $nS_L$  (number of segregating sites-by-length) (Ferrer-Admetlla et al. 2014) for individual populations (supplementary tables S5–S9, Supplementary Material online) and *xp-EHH* (cross population extended haplotype homozygosity) (Sabeti et al. 2007) for comparisons between population pairs. For individual populations, we focused on variants with  $|iHS|$  *P* values for <0.001 and  $|nS_L|$  values >2 (supplementary tables S5–S9, Supplementary Material online). GO-term analysis of the 82 genes tagged by these variants revealed an enrichment of genes in the categories “response to stress” and “response to stimulus” (*P* value after Bonferroni correction <0.001 and FDR <0.05) (fig. 6 and supplementary table S10, Supplementary Material online) We further confirmed this enrichment of GO-terms using a permutation method-based approach implemented in Gowinda (Kofler and Schlötterer 2012) (supplementary table S14, Supplementary Material online).

Consistent with the GO category enrichment, we noticed several NLR genes, a family that includes many known disease resistance genes (Van de Weyer et al. 2019). These included *RPP13* and *BAR1*, which confer resistance to the oomycete *Hyaloperonospora arabidopsidis* (*Har*) (Bittner-Eddy et al. 2000) and bacteria of the genus *Pseudomonas* (Laflamme et al. 2020). We measured the frequency of alternative haplotypes around these loci to determine the nature of the selective sweep (Garud et al. 2015). The most frequent haplotype is designated as  $H_1$  and the second most as  $H_2$ , from which a modified product of haplotype frequency ( $H_{12}$ ) and the  $H_2/H_1$  ratio are calculated. At *RPP13* and *BAR1*, we observed relatively low values for these two metrics and the presence of the selected alleles on multiple backgrounds, which together suggests soft sweeps at these loci (supplementary fig. S19A and B, Supplementary Material online). On the other hand, a pronounced hard sweep was observed in and around another putatively selected NLR, *BURNOUT1*, in the population OHML (supplementary fig. S19A and B, Supplementary Material online), with the selected allele found on a single haplotype. Similar to the  $|iHS|$  and  $|nS_L|$  results, genes with high *xp-EHH* scores included several genes known to be



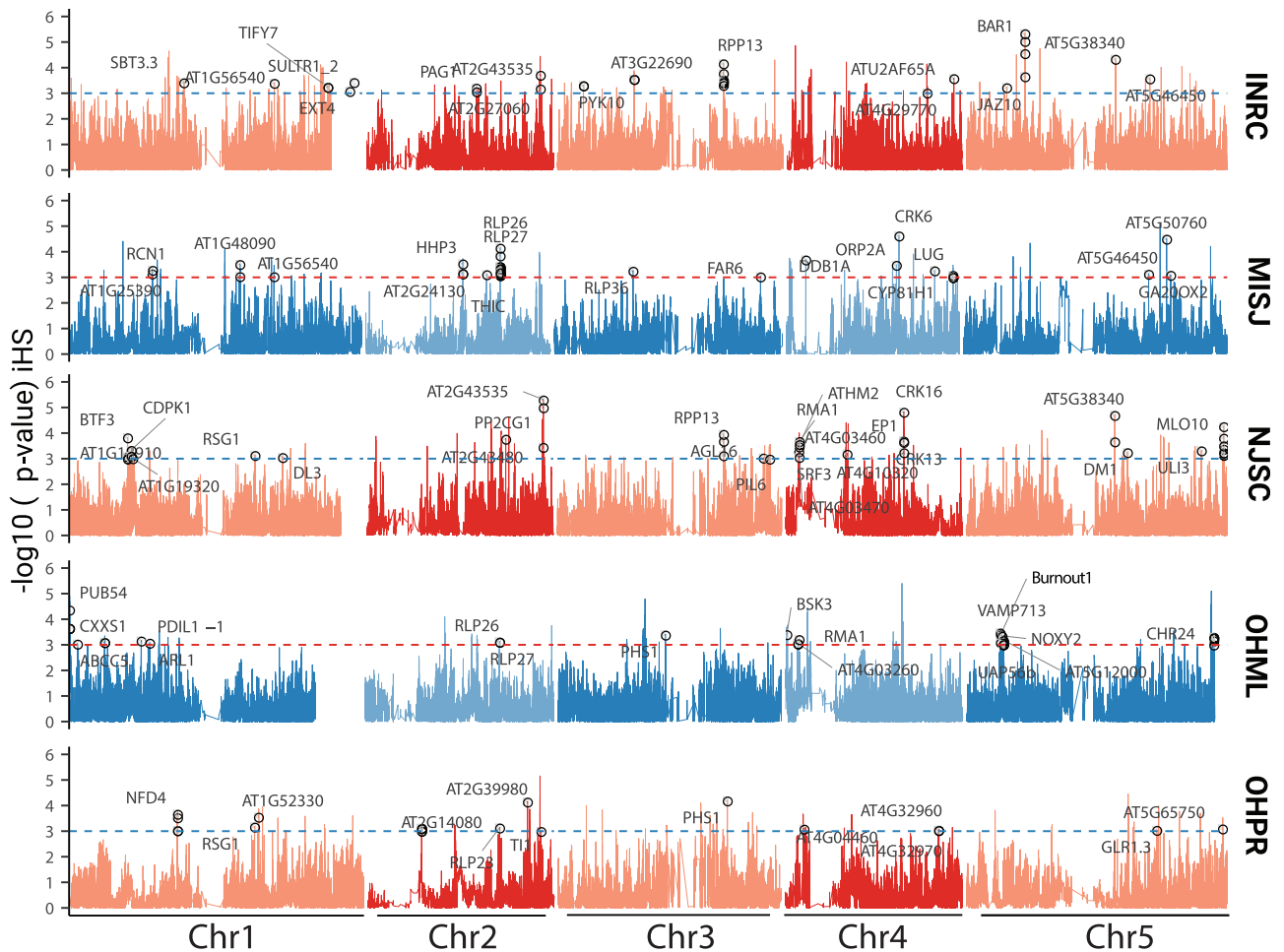


**Fig. 6.** Genome-wide haplotype-based selection statistics in five N. American populations. Genome-wide  $P$  values of  $|iHS|$  scores (based on empirical distribution). Dashed horizontal lines correspond to a  $P$  value significance threshold of 0.001. Selection candidates, which also had  $|nS_L|$  scores of  $>2$ , from the enriched GO categories of response to stress and response to stimulus (Fisher's exact test with Bonferroni correction,  $P$  value  $<0.001$  and FDR  $<0.05$ ) are plotted with gene names or gene IDs.

involved in biotic and abiotic stress responses (supplementary table S11, Supplementary Material online).

In order to obtain direct evidence of whether the positively selected alleles are entering the population through admixture, we used data collected for presence of disease symptoms of downy mildew caused by *Har* (details in Supplementary Material online) on the samples. We chose the MISJ population for this analysis because the rate of infection in this population was comparatively higher than others with many RAD-seq genotyped individuals (36 diseased and 115 healthy individuals based on visual observation at the time of collection, supplementary table S15, Supplementary Material online). We observed that the genetic differentiation measured by  $F_{ST}$  was higher on chromosome 4 between groups of diseased and healthy individuals (supplementary fig. S20A, Supplementary Material online). MISJ has admixed individuals from Hpg1 and OhioMich1 source groups (fig. 2 and supplementary fig. S6 and table S2, Supplementary Material online), therefore we calculated  $F_{ST}$  of the two groups with Hpg1 separately. We found that the healthy individuals were significantly differentiated to Hpg1 in the genomic region of 9–12 Mb of chromosome 4 compared with the diseased

individuals (supplementary fig. S20B, Supplementary Material online), whereas diseased individuals showed lower non-Hpg1 ancestry than the healthy individuals on chromosome 4 in general (supplementary fig. S20C, Supplementary Material online) and significantly lower non-Hpg1 local ancestry in the genomic region of 9–12 Mb (supplementary fig. S20D and E, Supplementary Material online). This genomic region is characterized by the presence of a well-known *Har* disease resistance gene cluster of *RPP4/5* (Noël et al. 1999; Holub 2001; van der Biezen et al. 2002). Thus, this result strongly suggests that *RPP4/5* genomic region from non-Hpg1 group OhioMich1 is preferentially kept in the MISJ population as it confers disease resistance.

## Discussion

How newly introduced, nonindigenous species adapt to new environments is a topic of long-standing interest in eco-evolutionary biology of invasive species (Baker and Stebbins 1965; Bock et al. 2015). There are two potential challenges facing invasive species: First, the niches in the new environment might be different from the ones in the native range

and/or already filled by other species. Second, introductions typically begin with few individuals and therefore potentially a narrow genetic basis. The initial lack of genetic diversity can be overcome by new mutations or through the generation of new genetic combinations, either by crosses among the introduced population or with close relatives that are present in and already adapted to the new environment. We have used *A. thaliana* to address these questions.

*Arabidopsis thaliana* is native to Europe, Asia, and Africa, where it is found mostly as a human commensal (Hoffmann 2002; 1001 Genomes Consortium 2016; Durvasula et al. 2017; Lee et al. 2017; Zou et al. 2017). The human-assisted expansion of this species to N. America presents an excellent system to study processes associated with colonization of a new environment because it occurred recently and because the genetic diversity in the native range is so well documented for *A. thaliana*. Previous work has laid the groundwork for our study, but was limited by a paucity of genetic markers (Platt et al. 2010) or a focus on a single-dominant lineage (Exposito-Alonso, Becker, et al. 2018). We have investigated multiple individuals from several N. American populations at the whole-genome level, allowing us to describe fine-scale haplotype sharing within N. America and between N. America and individuals from the native range, either sequenced as a part of the 1001 Genomes project (1001 Genomes Consortium 2016) or subsequent efforts focused on Africa (Durvasula et al. 2017), China (Zou et al. 2017), and Ireland (this work).

### Multiple Independent Introductions

The extant diversity among *A. thaliana* individuals in N. America can be traced back to multiple, almost certainly independent introductions of lineages of diverged ancestries from three distinct geographic regions of Western Europe (British Isles/Ireland, Upper and Eastern France), central Europe (Germany, Czechia, and Austria), and Eastern Europe (the Baltic region and Russia). We detected these introductions using methods based on haplotype sharing (Lawson et al. 2012), allele frequencies (Patterson et al. 2012), and rare-allele sharing (Schiffels et al. 2016; Flegontov et al. 2019), lending considerable confidence to our findings and illuminating the extant diversity from several different angles. Significantly, even though we confirm that North-Western Europe and specifically the British isles are a major source of multiple introductions, the predominant lineage Hpg1, which has been estimated to have been introduced ~400 years ago (Exposito-Alonso, Becker, et al. 2018), has more ancestry from Upper and Eastern France than from the British Isles. Its spread in N. America could be attributed to rapid expansion of French colonists from current Canada (then Acadia) along the Mississippi valley during the early period of post-Columbian colonization (Hamilton 1902). Our approach of haplotype-based clustering of individuals at different hierarchical levels using fineSTRUCTURE (Lawson et al. 2012) has allowed us to pinpoint several Western European sources of N. American *A. thaliana*. Although the sparse representation of individuals from Eastern Europe and Asia has limited our ability to more

precisely identify the source of introductions from these regions, it is clear that Eastern Europe has contributed to extant N. American *A. thaliana* ancestry. Historical patterns of human migration indicate that northern and western Europeans arrived in significant numbers from the 1840s to 1880s, followed by waves of southern and eastern Europeans from the 1880s to 1910s (Passel and Fix 1994), which are reflected in the genetic make-up of present-day humans in N. America (Bryc et al. 2015; Dai et al. 2020). In the regions where we collected *A. thaliana* in N. America, humans have more British, Irish, central and eastern European ancestry than western, southern, and northern European ancestry (Bryc et al. 2015), consistent with the *A. thaliana* ancestry patterns. Thus, local anthropogenic introduction of *A. thaliana* can be proposed as a parsimonious explanation for the presence of diverged lineages in the regions of N. America that we sampled in our study.

### Wide-Spread Admixture

Perhaps our most significant finding is how multiple introductions have led to present-day N. American *A. thaliana* being surprisingly genetically diverse, different from many other colonizing or invading species (Dlugosch and Parker 2008). This highlights how between-population variation in the native range has translated into within-population variation in N. America (Rius and Darling 2014). In organisms with low outcrossing rates such as *A. thaliana*, benefits of local adaptation in the native range hinder admixture from other populations, even in the face of inbreeding depression. It has been argued that during invasion of new territory, there is a temporary loss of local adaptation that not only lifts the maladaptive burden of admixture but even favors admixture (Verhoeven et al. 2011; Rius and Darling 2014). We indirectly observe this in AEA regions' geographically restricted haplotype-sharing patterns (supplementary fig. S24C, Supplementary Material online, quantified as Bray–Curtis distance in supplementary fig. S25, Supplementary Material online) whereas due to multiple introductions, N. American *A. thaliana* has a mixture of diverged ancestries (fig. 3A) and among some individuals levels of increased compositional dissimilarity (supplementary fig. S25, Supplementary Material online) similar to that seen in individuals from AEA regions. Further, compared with some AEA regions, nucleotide diversity ( $\pi$ ) and total derived allele count are elevated in a few N. American populations (supplementary fig. S26, Supplementary Material online). Patterns that are similar to the ones we have reported here for *A. thaliana* have been suggested for other systems, albeit mostly based on limited genetic information and without the benefit of being able to infer ancestry along each chromosome (Kolbe et al. 2004; Lavergne and Molofsky 2007; Facon et al. 2008; Smith et al. 2020).

Based on the observed lower selfing rates in N. America compared with Europe, it has been suggested that under slightly increased outcrossing, mixing of haplotypes should be expected (Platt et al. 2010). In line with this hypothesis, we observed that most N. American *A. thaliana* populations have individuals with admixture from the dominant Hpg1

*group*. Being apparently already well-adapted to the N. American ecological context upon its introduction, today Hpg1 is a wide-spread lineage in N. America (Platt et al. 2010; Exposito-Alonso, Becker, et al. 2018). Admixture with Hpg1, followed by selection, might have benefited and accelerated the spread of new incoming lineages. A case in support of this can be made for *groups* that are found in Indiana, where the human settlers in the mid-19th century came predominantly from North Carolina, Virginia, and Kentucky (Lynch 1915). Our demographic reconstructions using herbarium samples of SouthIndiana4 *group* estimated divergence times of 121 years-before present (126–119 HPD; 95%, supplementary fig. S21, Supplementary Material online) coincidental to the human migration and its admixture with Hpg1 has resulted in *groups* that are extant in North Carolina (our collection), Kentucky (1001 Genomes collection), and Georgia (herbarium collection). Alternative explanations such as short-term fitness benefits through heterosis (Facon et al. 2005; Keller and Taylor 2010) can currently not be ruled out, but could be tested with common garden experiments across N. American field sites. We also note that although some populations show richness in terms of haplotype diversity inferred with WGS (fig. 2) as a direct result of admixture events, our RAD-seq genotyping of over 2,000 individuals and coarse-scale haplotype ancestry and diversity estimates (supplementary figs. S22 and S23, Supplementary Material online) suggest that populations CTDE, CTPN, MAUR, and OHOS might have yet unexplored haplotype diversity.

### Purging of Deleterious Mutations

An important aspect of colonization is the severe genetic bottleneck due to founder effects and subsequent accumulation of deleterious mutations (Kirkpatrick and Jarne 2000; Verhoeven et al. 2011; Willi 2013; Schrieber and Lachmuth 2017), further exacerbated by predominant self-fertilization (Noël et al. 2017). One of the ways out of this invasion paradox (Estoup et al. 2016) might be admixture between colonizing lineages, which can both remove deleterious mutations (Heller and Maynard Smith 1978) and generate new genetic combinations that are only adaptive in the new environment (Dlugosch and Parker 2008; Rius and Darling 2014). Consistent with the expectation under admixture alone, we observed that the admixed N. American *A. thaliana* haplogroups have fewer fixed derived deleterious alleles. When background levels of reduction in fixed derived alleles using synonymous mutations were accounted for, we observed that compared with source *groups*, nonsynonymous tolerated mutations are removed at a lower rate than nonsynonymous deleterious mutations in the admixed *groups* (supplementary fig. S18D, Supplementary Material online). This demonstrates that admixture has been successful in removing some of the potential nonsynonymous mutational load carried by the founder lineages. A caveat is that the deleteriousness of variants is based on presumed reduction or loss of molecular function (Kono et al. 2018), even though gene inactivation can be adaptive as well (Olson 1999). A more direct approach to determining the extent of purging of mutational load in N. American colonizing lineages could

come from direct estimates of local adaptation deficits and selection coefficients, by comparing the fitness of N. American individuals at their site of collection against a global sample of *A. thaliana* accessions (Exposito-Alonso et al. 2019) or by quantifying the amount of genetic rescue or  $F_1$  heterosis in crosses between populations (Koski et al. 2019).

### Resistance Genes as Loci under Selection

An indication of selection having potentially shaped the geographic distribution of genetic diversity in N. American *A. thaliana* is the observation of environmental dissimilarity between N. American haplogroups and their source lineages from the native range being negatively correlated with shared ancestry between them. Given that *A. thaliana* is a human commensal in its native range, it is not hard to envision that anthropogenically induced adaptation to invade (AIAI) (Hufbauer et al. 2012) might play a significant role in having accelerated *A. thaliana*'s adaptation to the N. American environment.

If a species is far from an adaptive peak, large-effect mutations are particularly likely to affect the speed of adaptation (Fisher 1930). Although the relative importance of abiotic and biotic factors for adaptation is still debated (Morris et al. 2020), some of the most drastic effects arise from disease resistance genes, where single genes have outsized effects on fitness and survival on plants in the presence of pathogens. In *Capsella*, it has been shown that dramatic losses of genetic diversity after extreme genetic bottlenecks can be tolerated at most genes in the genome, except for immunity loci (Koenig et al. 2019). Our selection scans with *A. thaliana* individuals from five different N. American populations have revealed that genes related to biotic stress are enriched among selection candidates. These include genes known to have alleles that confer resistance to two of the most prominent pathogens of *A. thaliana*, *H. arabidopsidis*, and *Pseudomonas* (Holub and Beynon 1997; Karasov et al. 2014, 2018). One of the loci we found to be under selection is *RPP13* (Rose et al. 2004), whose product recognizes the coevolved, highly polymorphic effector ATR13 from *H. arabidopsidis* (Allen et al. 2004). Another one is *BAR1*, whose product recognizes members from the conserved HopB effector family from *Pseudomonas* (Lafamme et al. 2020). Although *RPP13* is under balancing selection in at least part of the native range (Allen et al. 2004), we observe that a specific *RPP13* allele is found on different haplotypes (supplementary fig. S28, Supplementary Material online), has a comparable nucleotide diversity to AEA ancestral source regions (supplementary fig. S29, Supplementary Material online) and has undergone a selective sweep in N. American *A. thaliana* populations. Given that *H. arabidopsidis* appears to be an *A. thaliana* specialist (Slusarenko and Schlaich 2003), it must have been introduced with its *A. thaliana* host, and its genetic diversity in the introduced range might be as low or even lower than that of its host, potentially providing an explanation for the apparent selective sweep at *RPP13*. Apart from haplotype homozygosity-based scans, we observed high differentiation in the *RPP4/5* region of the genome between individuals in the MISJ population that were or were not visibly infected with *H. arabidopsidis* when we

collected them. Local ancestry estimates confirm that this region of the genome has been entering the population through admixture and is of non-Hpg1 origin. As *RPP4/5* is known to harbor high levels of polymorphism and is known to be involved in frequency-dependent selection for resistance to *H. arabidopsidis* (Noël et al. 1999), this introgression event could be driven by positive selection against local strains of this pathogen.

## Conclusions

Altogether, our analysis using WGS from extant N. American *A. thaliana* has established a scenario of multiple introductions from sources of previously diverged Eurasian lineages. We provide evidence that new haplotype diversity has been generated through wide-spread admixture among introduced lineages, relieving mutational load and providing raw material for selection to act upon. Our findings are thus consistent with earlier proposals that hybridization can lead to the introduction of adaptive variation via introgression or admixture (Anderson 1948, 1949; Stebbins 1959; Grant 1981). The advent of molecular analyses has confirmed the relevance of hybridization for adaptation and speciation (Arnold 1996, 2004; Rieseberg 1997) and our observations are consistent with admixture being important for invasive success. Admixture can facilitate successful colonization when individuals from divergent populations have been recurrently introduced to a new range (Rius and Darling 2014; Dlugosch et al. 2015; Estoup et al. 2016). North American *A. thaliana* therefore may not have suffered from the genetic paradox of invasion (Allendorf and Lundquist 2003; Estoup et al. 2016). Finally, because *A. thaliana* has also colonized other continents, including S. America and Australia (Alonso-Blanco and Koornneef 2000; Kasulin et al. 2017), it will be interesting to determine both how genetic diversity of *A. thaliana* in these other places compares with N. America, and how genetic diversity of *A. thaliana* compares with that of other plants that have been inadvertently introduced to N. America by humans (Neuffer and Hurka 1999; Durka et al. 2005; La Sorte et al. 2007).

## Materials and Methods

### Sample Collection and Sequencing

Some samples were collected dried by pressing in acid-free paper with a wooden press for 8–12 weeks to produce herbarium samples. For other field samples, two to three well-expanded leaves were collected in a microcentrifuge tube and immediately placed on dry ice and kept at  $-80^{\circ}\text{C}$  until further processing. Seeds of Irish accessions were grown in the lab from seeds. Details of DNA extraction using different protocols and sequencing can be found in [Supplementary Material](#) online.

### Mapping and Variant Calling

Reads were mapped using *bwa-mem* (*bwa*-0.7.15) (Li and Durbin 2009) to the TAIR10 reference genome ([https://www.arabidopsis.org/download\\_files/Genes/TAIR10\\_genome\\_release/TAIR10\\_chromosome\\_files/TAIR10\\_chr\\_all.fas](https://www.arabidopsis.org/download_files/Genes/TAIR10_genome_release/TAIR10_chromosome_files/TAIR10_chr_all.fas), last

accessed September 13, 2021) and sorted using *samtools* v1.3 (Li and Durbin 2009). Reads from herbarium samples were additionally trimmed with *skewer* (v. 0.1.127) (Jiang et al. 2014) using default parameters and merged with *flash* (v. 1.2.11) (Magoč and Salzberg 2011) with a maximum overlapping value of 150 bp, prior to mapping. SNP calling was performed with the Genome Analysis Tool Kit (GATK) best practices with modifications for single-end reads (DePristo et al. 2011; Van der Auwera et al. 2013). GATK tools used are described in [supplementary methods, Supplementary Material](#) online, and detailed parameters can be found in the script provided in the accompanying repository. Strategy and procedure to include SNPs from remaining *A. thaliana* global diversity data set can be found in the [Supplementary Material](#) online.

### Estimation of Recombination Rates

Haplotype phasing for estimation of recombination rate was performed with *Shapelt2* (v2.r837) (Delaneau et al. 2013) on samples from this project and a subset of the 1001 Genomes project (1001 Genomes Consortium 2016). After phasing, the recombination rate variation along the chromosomes was estimated using *LDhelmet* v1.7 (Chan et al. 2012). Detailed procedure is described in the [supplementary methods, Supplementary Material](#) online.

### Population Genetic Analysis

#### PCA, UMAP, and IBD

Principal component analysis was performed using *SmartPCA* of *EIGENSOFT* version 6.0.1 (Patterson et al. 2006) package. We used the first 50 PCs as input for generating two UMAP embeddings using Python package *umap* v0.4.6 (McInnes et al. 2018). Details of the analyses are in the [supplementary methods, Supplementary Material](#) online. Identity-by-descent and identity-by-state analyses were carried out with *PLINK* v1.90 (Chang et al. 2015).

#### Chromosome Painting and Clustering

Clustering of individuals based on shared ancestry from haplotype data was performed using *fineSTRUCTURE* on a coancestry matrix derived with the software *CHROMOPAINTER* v2 (Lawson et al. 2012), which treats all the individuals (except the individual whose ancestry is being reconstructed) as donor haplotypes and generates a mosaic of shared chunks copied from these donors in a given recipient individual. Similarity in the patterns of shared chunks (copying vectors) is indicative of shared ancestry and is the basis of the model-based clustering approach taken by the *fineSTRUCTURE* algorithm. Specifically, we performed this analysis in the following hierarchical way:

- (1) All N. American individual haplotypes were painted as a mosaic of all other N. American individuals' haplotypes (self-excluding).
- (2) All non-N. American (Afro-Eur-Asian/AEA) haplotypes were formed as a mosaic of each other. Based on the haplotype sharing these individuals were then clustered and grouped into what we call *subclusters*, *clusters*

(comprising *subclusters*), and *regions* (comprising clusters representing specific geographical regions).

- (3) All N. American haplotypes were then formed as a mosaic of AEA haplotype clusters. Detailed description of the analysis is in the [supplementary methods, Supplementary Material](#) online.

#### Treemix Analysis

We determined the phylogenetic relationship among the N. American *groups* and among these *groups* and AEA *subclusters* as inferred by fineSTRUCTURE using Treemix v1.13 (Pickrell and Pritchard 2012). Details are in the [supplementary methods, Supplementary Material](#) online.

#### $f_3$ -Outgroup Analysis

To determine the extent of shared drift between the AEA subclusters (smallest fineSTRUCTURE grouping) and N. American haplogroups, we used  $f_3$ -outgroup tests as described (Patterson et al. 2012). N. American<sub>(i)</sub> AEA SubCluster<sub>(j)</sub>; Relicts (Fs12\_3) configuration was used and implementation of the test was carried out using R package “*admixr*” (Petr et al. 2019).

#### qpWave and D-Statistic Analyses

To determine the minimum number of ancestry waves from AEA regions (comprised different haplogroup *subclusters* defined by fineSTRUCTURE analyses), we used D-statistic and qpWave analyses from ADMIXTOOLS (Reich et al. 2012). Details of the tree configurations and outgroups can be found in the [Supplementary Material](#) online.

#### Rare Allele Sharing

About 1,039 AEA individuals that formed the fineSTRUCTURE *subclusters* were used as a reference panel to ascertain rare alleles and calculate RAS between AEA *subclusters* and N. American haplogroups. The input files were prepared with the tools from repository at (<https://github.com/stschiff/rarecoal-tools>, last accessed September 13, 2021) and the analysis was performed by the pipeline available at (<https://github.com/TCLamnidis/RAStools>, last accessed September 13, 2021). Minimum allele count of 2 and maximum allele count of 20 was used on the SNPs with less than 10% missing data. Alleles were polarized with the *A. lyrata* data.

#### Phylogenetic Methods

Bayesian phylogenetic analyses were carried out using BEAST v2.4.8 (Bouckaert et al. 2014) for *groups* Hpg1 and SouthIndiana4. Details of the substitution model and prior used are in the [Supplementary Material](#) online.

#### Local Ancestry Inference

We performed LAI for RAD-seq genotyped samples from population MISJ and WGS samples from MISJ, NJSC, OHML, and OHPR with Loter model (Dias-Alves et al. 2018). Exact parameters and individuals used as reference

source *groups* are described in the [Supplementary Material](#) online.

#### Genetic Differentiation in MISJ Population

We calculated genetic differentiation ( $F_{ST}$ ) between individuals that showed visible symptoms of infection by *H. arabidopsidis* (described in Koch and Slusarenko [1990]) at the time of collection and individuals were visibly healthy. Detailed strategy to determine the significance of the differentiation between the two groups is described in the [Supplementary Material](#) online.

#### Environmental Factor Analysis

Historical climate data from 1970 to 2000 were downloaded from WorldClim2.0 (Fick and Hijmans 2017) at 2.5-min resolution using Python library latlon-utils 0.0.5 (<https://github.com/Chilipp/latlon-utils>, last accessed September 13, 2021). Environmental variables average temperature (°C), precipitation (mm), solar radiation ( $\text{kJ m}^{-2} \text{day}^{-1}$ ), and water vapor pressure (kPa) were used for further analysis. Pairwise Euclidean distances of all the environmental variables were calculated for each N. American haplogroup to AEA *subclusters* (mean Latitude–Longitude of individuals in a given *subcluster* was used) and standardized values were used to model shared drift (measured by  $f_3$ -outgroup statistics) among N. American haplogroups and AEA *subclusters* as a function of the environmental variables using Bayesian multilevel (hierarchical) linear regression. Description of the priors and hyper-priors is in the [supplementary methods, Supplementary Material](#) online.

Projection of the N. American haplogroups in reduced dimension formed by standardized average temperature, precipitation, and vapor pressure was performed using uniform manifold approximation and projection (UMAP) (McInnes et al. 2018). Two independent runs of UMAP were performed with different random numbers. In both the runs default “Euclidean” distance was used to compute distances in high dimensional space. We further used Ward’s linkage function on UMAP embeddings to determine hierarchical clustering patterns in the data set based on Euclidean distance. Details of the scripts and notebooks used for the analysis are in the accompanying repository.

#### Estimation of Scaled Fixed-to-Total Derived Allele Ratio ( $\Phi$ ) for N. American Groups across Mutational Categories

Ancestral state of the positions was determined using pairwise alignments between *A. thaliana* and outgroups *A. halleri* and *A. lyrata* ([ftp://ftp.ensemblgenomes.org/pub/plants/release-44/maf/ensembl-compara/pairwise\\_alignments/](ftp://ftp.ensemblgenomes.org/pub/plants/release-44/maf/ensembl-compara/pairwise_alignments/), last accessed September 13, 2021). The detailed strategy is described in the [supplementary methods, Supplementary Material](#) online. Precomputed SIFT 4G predictions for *A. thaliana* were obtained from ([https://sift.bii.a-star.edu.sg/sift4g/public//Arabidopsis\\_thaliana/](https://sift.bii.a-star.edu.sg/sift4g/public//Arabidopsis_thaliana/), last accessed September 13, 2021). Using these predictions, positions were divided into three different categories: 1) High-confidence deleterious

mutations (score = 0–0.05), 2) Nonsynonymous tolerated mutations (score = 0.05–1) and, 3) synonymous mutations. We then calculated the ratio of fixed-to-total derived alleles ( $\phi_{category}$ ) in every group separately for all categories (frequency of fixed alleles=1). We also calculated the genome-wide ratio of fixed-to-total derived alleles ( $\phi_{genome}$ ).  $\phi$  is influenced by the increase in effective population size as a result of admixture between the source *groups* and divergence. To account for this in comparisons among *groups*, we scaled  $\phi$  for high-confidence deleterious and for nonsynonymous tolerated mutations by dividing it with  $\phi$  calculated for synonymous mutations for individual groups:

$$\Phi_{category} = \frac{\phi_{category}}{\phi_{syn-tol}}$$

In addition to the scaling with synonymous variation we separately scaled the ratio with genome-wide fixed-to-total derived alleles ratio (using all the derived variation).

### Genome-Wide Selection Scans

We performed haplotype homozygosity-based selection scans to detect recent and ongoing selection. *iHS* (integrated haplotype score) (Voight et al. 2006) and XP-EHH (cross-population extended haplotype homozygosity) (Sabeti et al. 2007) were calculated using hapbin (Maclean et al. 2015), details are described in the [supplementary methods, Supplementary Material](#) online. Recombination map generated earlier was used in the estimation of both the statistics.  $nS_L$  (number of segregating sites by length) (Ferrer-Admetlla et al. 2014), Garud's H1, H12, and H2/H1 (Garud et al. 2015) (window size=500, step size=10), Tajima's *D* (window size = 50,000 and step size = 5,000) were calculated with scikit-allel (Miles et al. 2020). Nucleotide diversity for the population was calculated using a pipeline described by (Martin et al. 2015).

*iHS* and  $nS_L$  were used in a complementary manner. As *iHS* is known to be affected by recombination rate variation (O'Reilly et al. 2008), we used *iHS* first, and based on empirical distribution of the scores, *P* values were calculated per SNP.  $nS_L$  was then calculated on the same data set. As  $nS_L$  is robust to variation in mutation and recombination rates (Ferrer-Admetlla et al. 2014), overlap of the SNPs that showed *iHS* *P* value less than 0.001 and  $nS_L$  higher than 2 was taken as a signal of selection. GO-term analysis of the genes carrying the candidate selected SNPs was performed with AgriGOv2 (Tian et al. 2017) with PlantGo-Slim categories. For enrichment of GO terms, Fisher's exact test with Bonferroni correction was used. We also performed GO-term enrichment analysis using a permutation-based method implemented in Gowinda v1.12 (Kofler and Schlötterer 2012) because it takes into account gene clustering and size.

### Supplementary Material

[Supplementary data](#) are available at *Molecular Biology and Evolution* online.

### Acknowledgments

We thank Rebecca Schwab for help with organizing first collection trip; Claudia Friedemann, Cathy Herring (NCSU Central Crops Research Station), Carol Ann McCormick (University of North Carolina), Jon Peter (New York Botanical Garden), Nelson Garcia (Rutgers University), Rosa Raudales and Sanjukta Majumder (University of Connecticut), Robert Capers (George Safford Torey Herbarium), Irina Kadis and Alexei Zinovjev (Arnold Arboretum), Jason Parrish, Jiangbo Fan, Guo-Liang Wang, Lynn Jin, David Mackey, Maria Bellizzi, and John Freudenstein (Ohio State University), Neville Millar (Kellogg Biological Station), Eric Knox (Indiana University), Timothy Morton and Joy Bergelson (University of Chicago), Alan Fryday, Bethany Huot, and Sheng Yang He (Michigan State University), and Christine Niezgodna (Field Museum of Natural History) for help during sample collection; Suresh Balasubramanian (Monash University) for seeds of Irish accessions; Sang-Tae Kim, Julian Regalado, Dino Jolic, Danelle Seymour, Jörg Hagmann, and Jorge Quintana for help with setting up the RAD-seq analysis pipeline and for help throughout the project; Christa Lanz, Julia Hildebrandt for help with sequencing; and Stephan Schiffels (MPI for Science of Human History), Talia Karasov, and Richard Neher for discussions. We thank anonymous reviewers for their constructive comments that helped make substantial improvements to the manuscript. This work was funded by the Deutsche Forschungsgemeinschaft (DFG) through ERA-CAPS Project 1001GenomesPlus and the Max Planck Society.

### Author Contributions

G.S., J.D., and D.W. conceived the project. G.S. and J.D. organized the collection trips. G.S. and J.D. collected the samples. G.S., J.D., A.B., M.Q.D., A.G.H., and D.S.L. processed the samples for sequencing and performed DNA extractions. G.S., J.D., and A.B. prepared sequencing libraries. G.S. and J.D. scripted and ran sequence processing pipelines. G.S. performed formal analysis. H.A.B., C.B.F., and D.W. supervised the research. G.S. wrote the original draft. G.S., S.M.L., D.S.L., C.B.F., H.A.B., and D.W. reviewed and edited the draft.

### Data Availability

Code and high-resolution images from the main text are available from [https://github.com/weigelworld/north\\_american\\_arabidopsi](https://github.com/weigelworld/north_american_arabidopsi) (last accessed September 13, 2021) repository. Short reads have been deposited in the European Nucleotide Archive under the accession number PRJEB42417.

### References

- 1001 Genomes Consortium. 2016. 1,135 genomes reveal the global pattern of polymorphism in *Arabidopsis thaliana*. *Cell* 166:481–491.
- Allen RL, Bitner-Eddy PD, Grenville-Briggs LJ, Meitz JC, Rehmany AP, Rose LE, Beynon JL. 2004. Host-parasite coevolutionary conflict between *Arabidopsis* and downy mildew. *Science* 306(5703):1957–1960.
- Allendorf FW, Lundquist LL. 2003. Introduction: population biology, evolution, and control of invasive species. *Conserv Biol.* 17(1):24–30.

- Alonso-Blanco C, Koornneef M. 2000. Naturally occurring variation in *Arabidopsis*: an underexploited resource for plant genetics. *Trends Plant Sci.* 5(1):22–29.
- Anderson E. 1948. Hybridization of the habitat. *Evolution* 2(1):1–9.
- Anderson E. 1949. Introgressive hybridization. New York: J. Wiley.
- Arnold B, Corbett-Detig RB, Hartl D, Bomblies K. 2013. RADseq underestimates diversity and introduces genealogical biases due to non-random haplotype sampling. *Mol Ecol.* 22(11):3179–3190.
- Arnold ML. 1996. Natural hybridization and introgression. Princeton (NJ): Princeton University Press.
- Arnold ML. 2004. Transfer and origin of adaptations through natural hybridization: were Anderson and Stebbins right? *Plant Cell* 16(3):562–570.
- Baker HG, Stebbins GL. 1965. The genetics of colonizing species: proceedings. New York: Academic Press.
- Bitner-Eddy PD, Crute IR, Holub EB, Beynon JL. 2000. RPP13 is a simple locus in *Arabidopsis thaliana* for alleles that specify downy mildew resistance to different avirulence determinants in *Peronospora parasitica*. *Plant J.* 21(2):177–188.
- Bock DG, Caseys C, Cousens RD, Hahn MA, Heredia SM, Hübner S, Turner KG, Whitney KD, Rieseberg LH. 2015. What we still don't know about invasion genetics. *Mol Ecol.* 24(9):2277–2297.
- Bouckaert R, Heled J, Kühnert D, Vaughan T, Wu C-H, Xie D, Suchard MA, Rambaut A, Drummond AJ. 2014. BEAST 2: a software platform for Bayesian evolutionary analysis. *PLoS Comput Biol.* 10(4):e1003537.
- Bryc K, Durand EY, Macpherson JM, Reich D, Mountain JL. 2015. The genetic ancestry of African Americans, Latinos, and European Americans across the United States. *Am J Hum Genet.* 96(1):37–53.
- Busby GB, Helleenthal G, Montinaro F, Tofaneli S, Bulayeva K, Rudan I, Zemunik T, Hayward C, Toncheva D, Karachanak-Yankova S, et al. 2015. The role of recent admixture in forming the contemporary West Eurasian genomic landscape. *Curr Biol.* 25(19):2518–2526.
- Cariou M, Duret L, Charlat S. 2016. How and how much does RAD-seq bias genetic diversity estimates? *BMC Evol Biol.* 16(1):240.
- Chan AH, Jenkins PA, Song YS. 2012. Genome-wide fine-scale recombination rate variation in *Drosophila melanogaster*. *PLoS Genet.* 8(12):e1003090.
- Chang CC, Chow CC, Tellier LC, Vattikuti S, Purcell SM, Lee JJ. 2015. Second-generation PLINK: rising to the challenge of larger and richer datasets. *Gigascience* 4:7.
- Colautti RI, Lau JA. 2015. Contemporary evolution during invasion: evidence for differentiation, natural selection, and local adaptation. *Mol Ecol.* 24(9):1999–2017.
- Dai CL, Vazifteh MM, Yeang C-H, Tachet R, Wells RS, Vilar MG, Daly MJ, Ratti C, Martin AR. 2020. Population histories of the United States revealed through fine-scale migration and haplotype analysis. *Am J Hum Genet.* 106(3):371–388.
- Delaneau O, Howie B, Cox AJ, Zagury J-F, Marchini J. 2013. Haplotype estimation using sequencing reads. *Am J Hum Genet.* 93(4):687–696.
- DePristo MA, Banks E, Poplin R, Garimella KV, Maguire JR, Hartl C, Philippakis AA, del Angel G, Rivas MA, Hanna M, et al. 2011. A framework for variation discovery and genotyping using next-generation DNA sequencing data. *Nat Genet.* 43(5):491–498.
- Dias-Alves T, Mairal J, Blum MGB. 2018. Loter: a software package to infer local ancestry for a wide range of species. *Mol Biol Evol.* 35(9):2318–2326.
- Dlugosch KM, Anderson SR, Braasch J, Cang FA, Gillette HD. 2015. The devil is in the details: genetic variation in introduced populations and its contributions to invasion. *Mol Ecol.* 24(9):2095–2111.
- Dlugosch KM, Parker IM. 2008. Founding events in species invasions: genetic variation, adaptive evolution, and the role of multiple introductions. *Mol Ecol.* 17(1):431–449.
- Durka W, Bossdorf O, Prati D, Auge H. 2005. Molecular evidence for multiple introductions of garlic mustard (*Alliaria petiolata*, Brassicaceae) to North America. *Mol Ecol.* 14(6):1697–1706.
- Durvasula A, Fulgione A, Gutaker RM, Alacakaptan SI, Flood PJ, Neto C, Tsuchimatsu T, Burbano HA, Xavier Picó F, Alonso-Blanco C, et al. 2017. African genomes illuminate the early history and transition to selfing in *Arabidopsis thaliana*. *Proc Natl Acad Sci U S A.* 114(20):5213–5218.
- Ebenesersdóttir SS, Sandoval-Velasco M, Gunnarsdóttir ED, Jagadeesan A, Gumundsdóttir VB, Thordardóttir EL, Einarsdóttir MS, Moore KHS, Sigursson Á, Magnúsdóttir DN, et al. 2018. Ancient genomes from Iceland reveal the making of a human population. *Science* 360(6392):1028–1032.
- Estoup A, Ravigné V, Hufbauer R, Vitalis R, Gautier M, Facon B. 2016. Is there a genetic paradox of biological invasion? *Annu Rev Ecol Evol Syst.* 47(1):51–72.
- Exposito-Alonso M, Becker C, Schuenemann VJ, Reiter E, Setzer C, Slovak R, Brachi B, Hagemann J, Grimm DG, Chen J, et al. 2018. The rate and potential relevance of new mutations in a colonizing plant lineage. *PLoS Genet.* 14(2):e1007155.
- Exposito-Alonso M, Exposito-Alonso M, Gómez Rodríguez R, Barragán C, Capovilla G, Chae E, Devos J, Dogan ES, Friedemann C, Gross C, et al. 2019. Natural selection on the *Arabidopsis thaliana* genome in present and future climates. *Nature [Internet].* 573(7772):126–129.
- Exposito-Alonso M, Vasseur F, Ding W, Wang G, Burbano HA, Weigel D. 2018. Genomic basis and evolutionary potential for extreme drought adaptation in *Arabidopsis thaliana*. *Nat Ecol Evol.* 2(2):352–358.
- Facon B, Jarne P, Pointier JP, David P. 2005. Hybridization and invasiveness in the freshwater snail *Melanoides tuberculata*: hybrid vigour is more important than increase in genetic variance. *J Evol Biol.* 18(3):524–535.
- Facon B, Pointier J-P, Jarne P, Sarda V, David P. 2008. High genetic variance in life-history strategies within invasive populations by way of multiple introductions. *Curr Biol.* 18(5):363–367.
- Ferrer-Admetlla A, Liang M, Korneliusen T, Nielsen R. 2014. On detecting incomplete soft or hard selective sweeps using haplotype structure. *Mol Biol Evol.* 31(5):1275–1291.
- Fick SE, Hijmans RJ. 2017. WorldClim 2: new 1-km spatial resolution climate surfaces for global land areas. *Int J Climatol.* 37(12):4302–4315.
- Fisher RA. 1930. The genetical theory of natural selection. Oxford: Clarendon Press.
- Flegontov P, Altınışık NE, Changmai P, Rohland N, Mallick S, Adamski N, Bolnick DA, Broomandkhoshbacht N, Candilio F, Culleton BJ, et al. 2019. Palaeo-Eskimo genetic ancestry and the peopling of Chukotka and North America. *Nature* 570(7760):236–240.
- Fulgione A, Hancock AM. 2018. Archaic lineages broaden our view on the history of *Arabidopsis thaliana*. *New Phytol.* 219(4):1194–1198.
- Fulgione A, Koornneef M, Roux F, Hermisson J, Hancock AM. 2018. Madeiran *Arabidopsis thaliana* reveals ancient long-range colonization and clarifies demography in Eurasia. *Mol Biol Evol.* 35(3):564–574.
- Garud NR, Messer PW, Buzbas EO, Petrov DA. 2015. Recent selective sweeps in North American *Drosophila melanogaster* show signatures of soft sweeps. *PLoS Genet.* 11(2):e1005004.
- Gelman A. 2006. Multilevel (hierarchical) modeling: what it can and cannot do. *Technometrics* 48(3):432–435.
- Grant V. 1981. Plant speciation. New York City (NY): Columbia University Press.
- Green RE, Krause J, Briggs AW, Maricic T, Stenzel U, Kircher M, Patterson N, Li H, Zhai W, Fritz MH-Y, et al. 2010. A draft sequence of the Neandertal genome. *Science* 328(5979):710–722.
- Hamilton PJ. 1902. The French settlement of the Mississippi valley. *Amer Hist Mag Tenn Hist Soc Quart.* 7:136–147.
- Heller R, Maynard Smith J. 1978. Does Muller's ratchet work with selfing? *Genet Res.* 32(3):289–293.
- Hoffmann MH. 2002. Biogeography of *Arabidopsis thaliana* (L.) Heynh. (Brassicaceae). *J Biogeography.* 29(1):125–134.
- Holub EB. 2001. The arms race is ancient history in *Arabidopsis*, the wildflower. *Nat Rev Genet.* 2(7):516–527.
- Holub EB, Beynon JL. 1997. Symbiology of mouse-ear cress (*Arabidopsis thaliana*) and oomycetes. In: Andrews JH, Tommerup IC, Callow JA, editors. Advances in botanical research. Vol. 24. Cambridge (MA): Academic Press. p. 227–273.

- Hsu C-W, Lo C-Y, Lee C-R. 2019. On the postglacial spread of human commensal *Arabidopsis thaliana*: journey to the East. *New Phytol.* 222(3):1447–1457.
- Hufbauer RA, Facon B, Ravigné V, Turgeon J, Foucaud J, Lee CE, Rey O, Estoup A. 2012. Anthropogenically induced adaptation to invade (AIAl): contemporary adaptation to human-altered habitats within the native range can promote invasions. *Evol Appl.* 5(1):89–101.
- Jiang H, Lei R, Ding S-W, Zhu S. 2014. Skewer: a fast and accurate adapter trimmer for next-generation sequencing paired-end reads. *BMC Bioinformatics* 15:182.
- Karasov TL, Almario J, Friedemann C, Ding W, Giolai M, Heavens D, Kersten S, Lundberg DS, Neumann M, Regalado J, et al. 2018. *Arabidopsis thaliana* and *Pseudomonas* pathogens exhibit stable associations over evolutionary timescales. *Cell Host Microbe.* 24(1):168–179.e4.
- Karasov TL, Kniskern JM, Gao L, DeYoung BJ, Ding J, Dubiella U, Lastra RO, Nallu S, Roux F, Innes RW, et al. 2014. The long-term maintenance of a resistance polymorphism through diffuse interactions. *Nature* 512(7515):436–440.
- Kasulin L, Rowan B, León RJC, Schuenemann VJ, Weigel D, Botto JF. 2017. A single haplotype hyposensitive to light and requiring strong vernalization dominates *Arabidopsis thaliana* populations in Patagonia, Argentina. *Mol Ecol.* 26(13):3389–3404.
- Keller SR, Taylor DR. 2010. Genomic admixture increases fitness during a biological invasion. *J Evol Biol.* 23(8):1720–1731.
- Kirkpatrick M, Jarne P. 2000. The effects of a bottleneck on inbreeding depression and the genetic load. *Am Nat.* 155(2):154–167.
- Koch E, Slusarenko A. 1990. *Arabidopsis* is susceptible to infection by a downy mildew fungus. *Plant Cell* 2(5):437–445.
- Koenig D, Hagemann J, Li R, Bemf F, Slotte T, Neuffer B, Wright SJ, Weigel D. 2019. Long-term balancing selection drives evolution of immunity genes in *Capsella*. *Elife [Internet]*. 8:e43606. Available from: <http://doi.org/10.7554/eLife.43606>.
- Kofler R, Schlötterer C. 2012. GOWINDA: unbiased analysis of gene set enrichment for genome-wide association studies. *Bioinformatics* 28(15):2084–2085.
- Kolbe JJ, Glor RE, Rodríguez Schettino L, Lara AC, Larson A, Losos JB. 2004. Genetic variation increases during biological invasion by a Cuban lizard. *Nature* 431(7005):177–181.
- Kono TJ, Lei L, Shih C-H, Hoffman PJ, Morrell PL, Fay JC. 2018. Comparative genomics approaches accurately predict deleterious variants in plants. *G3 (Bethesda)* 8(10):3321–3329.
- Koski MH, Layman NC, Prior CJ, Busch JW, Galloway LF. 2019. Selfing ability and drift load evolve with range expansion. *Evol Lett.* 3(5):500–512.
- Kumar P, Henikoff S, Ng PC. 2009. Predicting the effects of coding non-synonymous variants on protein function using the SIFT algorithm. *Nat Protoc.* 4(7):1073–1081.
- Lafamme B, Dillon MM, Martel A, Almeida RND, Desveaux D, Guttman DS. 2020. The pan-genome effector-triggered immunity landscape of a host-pathogen interaction. *Science* 367(6479):763–768.
- La Sorte FA, McKinney ML, Pyšek P. 2007. Compositional similarity among urban floras within and across continents: biogeographical consequences of human-mediated biotic interchange: intercontinental compositional similarity. *Glob Chang Biol.* 13(4):913–921.
- Lavergne S, Molofsky J. 2007. Increased genetic variation and evolutionary potential drive the success of an invasive grass. *Proc Natl Acad Sci U S A.* 104(10):3883–3888.
- Lawson DJ, Hellenthal G, Myers S, Falush D. 2012. Inference of population structure using dense haplotype data. *PLoS Genet.* 8(1):e1002453.
- Lee C-R, Svardal H, Farlow A, Exposito-Alonso M, Ding W, Novikova P, Alonso-Blanco C, Weigel D, Nordborg M. 2017. On the post-glacial spread of human commensal *Arabidopsis thaliana*. *Nat Commun.* 8:14458.
- Leslie S, Winney B, Hellenthal G, Davison D, Boumertit A, Day T, Hutnik K, Royrvik EC, Cunliffe B, Lawson DJ, et al. 2015. The fine-scale genetic structure of the British population. *Nature* 519(7543):309–314,
- Li H, Durbin R. 2009. Fast and accurate short read alignment with Burrows–Wheeler transform. *Bioinformatics* 25(14):1754–1760.
- Lowry DB, Hoban S, Kelley JL, Lotterhos KE, Reed LK, Antolin MF, Storfer A. 2017. Breaking RAD: an evaluation of the utility of restriction site-associated DNA sequencing for genome scans of adaptation. *Mol Ecol Resour.* 17(2):142–152.
- Lynch WO. 1915. The flow of colonists to and from Indiana before the civil war. *Indiana Mag Hist.* 11:1–7.
- Maclean CA, Chue Hong NP, Prendergast JGD. 2015. hapbin: an efficient program for performing haplotype-based scans for positive selection in large genomic datasets. *Mol Biol Evol.* 32(11):3027–3029.
- Magoč T, Salzberg SL. 2011. FLASH: fast length adjustment of short reads to improve genome assemblies. *Bioinformatics* 27(21):2957–2963.
- Martin SH, Davey JW, Jiggins CD. 2015. Evaluating the use of ABBA-BABA statistics to locate introgressed loci. *Mol Biol Evol.* 32(1):244–257.
- McInnes L, Healy J, Saul N, Großberger L. 2018. UMAP: Uniform manifold approximation and projection. *J Open Source Softw.* 3:861.
- Miles A, Bot P. I, Rodrigues MF, Ralph P, Harding N, Pisupati R, Rae S. 2020. cggh/scikit-allele: v1.3.1. Available from: <https://zenodo.org/record/3935797>. Accessed September 13, 2021.
- Miller MR, Dunham JP, Amores A, Cresko WA, Johnson EA. 2007. Rapid and cost-effective polymorphism identification and genotyping using restriction site associated DNA (RAD) markers. *Genome Res.* 17(2):240–248.
- Moest M, Van Belleghem SM, James JE, Salazar C, Martin SH, Barker SL, Moreira GRP, Mérot C, Joron M, Nadeau NJ, et al. 2020. Selective sweeps on novel and introgressed variation shape mimicry loci in a butterfly adaptive radiation. *PLoS Biol.* 18(2):e3000597.
- Montinaro F, Busby GBJ, Pascali VL, Myers S, Hellenthal G, Capelli C. 2015. Unravelling the hidden ancestry of American admixed populations. *Nat Commun.* 6:6596.
- Morris WF, Ehrlén J, Dahlgren JP, Loomis AK, Louthan AM. 2020. Biotic and anthropogenic forces rival climatic/abiotic factors in determining global plant population growth and fitness. *Proc Natl Acad Sci U S A.* 117(2):1107–1112.
- Neuffer B, Hurka H. 1999. Colonization history and introduction dynamics of *Capsella bursa-pastoris* (Brassicaceae) in North America: isozymes and quantitative traits. *Mol Ecol.* 8(10):1667–1681.
- Noël E, Jarne P, Glémin S, MacKenzie A, Segard A, Sarda V, David P. 2017. Experimental evidence for the negative effects of self-fertilization on the adaptive potential of populations. *Curr Biol.* 27(2):237–242.
- Noël L, Moores TL, van Der Biezen EA, Parniske M, Daniels MJ, Parker JE, Jones JD. 1999. Pronounced intraspecific haplotype divergence at the RPP5 complex disease resistance locus of *Arabidopsis*. *Plant Cell* 11(11):2099–2112.
- Olson MV. 1999. When less is more: gene loss as an engine of evolutionary change. *Am J Hum Genet.* 64(1):18–23.
- O'Reilly PF, Birney E, Balding DJ. 2008. Confounding between recombination and selection, and the Ped/Pop method for detecting selection. *Genome Res.* 18(8):1304–1313.
- Passel JS, Fix M. 1994. US immigration in a global context. *Indiana J Glob Leg Stud.* 2:5–19.
- Patterson N, Moorjani P, Luo Y, Mallick S, Rohland N, Zhan Y, Genschoreck T, Webster T, Reich D. 2012. Ancient admixture in human history. *Genetics* 192(3):1065–1093.
- Patterson N, Price AL, Reich D. 2006. Population structure and eigenanalysis. *PLoS Genet.* 2(12):e190.
- Peischl S, Dupanloup I, Kirkpatrick M, Excoffier L. 2013. On the accumulation of deleterious mutations during range expansions. *Mol Ecol.* 22(24):5972–5982.
- Petr M, Vernot B, Kelso J. 2019. admixr-R package for reproducible analyses using ADMIXTOOLS. *Bioinformatics* 35(17):3194–3195.
- Pickrell JK, Pritchard JK. 2012. Inference of population splits and mixtures from genome-wide allele frequency data. *PLoS Genet.* 8(11):e1002967.
- Platt A, Horton M, Huang YS, Li Y, Anastasio AE, Mulyati NW, Agren J, Bosssdorf O, Byers D, Donohue K, et al. 2010. The scale of population structure in *Arabidopsis thaliana*. *PLoS Genet.* 6(2):e1000843.



- Raghavan M, Skoglund P, Graf KE, Metspalu M, Albrechtsen A, Moltke I, Rasmussen S, Stafford TW, Jr, Orlando L, Metspalu E, et al. 2014. Upper Palaeolithic Siberian genome reveals dual ancestry of Native Americans. *Nature* 505(7481):87–91.
- Rédei GP. 1992. A heuristic glance at the past of *Arabidopsis* genetics. In: Koncz, C Chua, N-HSchell J, editors. *Methods in Arabidopsis research*. Singapore: World Scientific. p. 1–15.
- Reich D, Patterson N, Campbell D, Tandon A, Mazieres S, Ray N, Parra MV, Rojas W, Duque C, Mesa N, et al. 2012. Reconstructing Native American population history. *Nature* 488(7411):370–374.
- Rieseberg LH. 1997. Hybrid origins of plant species. *Annu Rev Ecol Syst.* 28(1):359–389.
- Rius M, Darling JA. 2014. How important is intraspecific genetic admixture to the success of colonising populations? *Trends Ecol Evol.* 29(4):233–242.
- Rose LE, Bittner-Eddy PD, Langley CH, Holub EB, Michelmore RW, Beynon JL. 2004. The maintenance of extreme amino acid diversity at the disease resistance gene, RPP13, in *Arabidopsis thaliana*. *Genetics* 166(3):1517–1527.
- Sabeti PC, Varilly P, Fry B, Lohmueller J, Hostetter E, Cotsapas C, Xie X, Byrne EH, McCarroll SA, Gaudet R, et al. 2007. Genome-wide detection and characterization of positive selection in human populations. *Nature* 449(7164):913–918.
- Schiffels S, Haak W, Paajanen P, Llamas B, Popescu E, Loe L, Clarke R, Lyons A, Mortimer R, Sayer D, et al. 2016. Iron Age and Anglo-Saxon genomes from East England reveal British migration history. *Nat Commun.* 7:10408.
- Schmickl R, Jørgensen MH, Brysting AK, Koch MA. 2010. The evolutionary history of the *Arabidopsis lyrata* complex: a hybrid in the amphiberian area closes a large distribution gap and builds up a genetic barrier. *BMC Evol Biol.* 10:98.
- Schrieber K, Lachmuth S. 2017. The Genetic Paradox of Invasions revisited: the potential role of inbreeding × environment interactions in invasion success: the Genetic Paradox revisited. *Biol Rev Camb Philos Soc.* 92(2):939–952.
- Slusarenko AJ, Schlaich NL. 2003. Downy mildew of *Arabidopsis thaliana* caused by *Hyaloperonospora parasitica* (formerly *Peronospora parasitica*). *Mol Plant Pathol.* 4(3):159–170.
- Smith AL, Hodkinson TR, Villellas J, Catford JA, Csergő AM, Blomberg SP, Crone EE, Ehrlén J, Garcia MB, Laine A-L, et al. 2020. Global gene flow releases invasive plants from environmental constraints on genetic diversity. *Proc Natl Acad Sci U S A.* 117(8):4218–4227.
- Smith JM, Haigh J. 1974. The hitch-hiking effect of a favourable gene. *Genet Res.* 23(1):23–35.
- Stebbins GL. 1959. The role of hybridisation in evolution. *Proc Am Philos Soc.* 103:231–251.
- Stephan W. 2019. Selective sweeps. *Genetics* 211(1):5–13.
- Tian T, Liu Y, Yan H, You Q, Yi X, Du Z, Xu W, Su Z. 2017. agriGO v2.0: a GO analysis toolkit for the agricultural community, 2017 update. *Nucleic Acids Res.* 45(W1):W122–W129.
- Van de Weyer A-L, Monteiro F, Furzer OJ, Nishimura MT, Cevik V, Witek K, Jones JDG, Dangl JL, Weigel D, Bemm F. 2019. A species-wide inventory of NLR genes and alleles in *Arabidopsis thaliana*. *Cell* 178(5):1260–1272.e14.
- Van der Auwera GA, Carneiro MO, Hartl C, Poplin R, Del Angel G, Levy-Moonshine A, Jordan T, Shakir K, Roazen D, Thibault J, et al. 2013. From FastQ data to high confidence variant calls: the Genome Analysis Toolkit best practices pipeline. *Curr Protoc Bioinformatics.* 43:11.10.1–11.10.33.
- van der Biezen EA, Freddie CT, Kahn K, Parker JE, Jones JDG. 2002. *Arabidopsis* RPP4 is a member of the RPP5 multigene family of TIR-NB-LRR genes and confers downy mildew resistance through multiple signalling components. *Plant J.* 29(4):439–451.
- Vatsiou AI, Bazin E, Gaggiotti OE. 2016. Detection of selective sweeps in structured populations: a comparison of recent methods. *Mol Ecol.* 25(1):89–103.
- Verhoeven KJF, Macel M, Wolfe LM, Biere A. 2011. Population admixture, biological invasions and the balance between local adaptation and inbreeding depression. *Proc Biol Sci.* 278(1702):2–8.
- Voight BF, Kudaravalli S, Wen X, Pritchard JK. 2006. A map of recent positive selection in the human genome. *PLoS Biol.* 4(3):e72.
- Walsh B, Lynch M. 2018. *Evolution and selection of quantitative traits*. Sunderland (MA): Oxford University Press.
- Willi Y. 2013. Mutational meltdown in selfing *Arabidopsis lyrata*. *Evolution* 67(3):806–815.
- Winter M, Kühn I, La Sorte FA, Schweiger O, Nentwig W, Klotz S. 2010. The role of non-native plants and vertebrates in defining patterns of compositional dissimilarity within and across continents: compositional dissimilarity at large scales. *Glob Ecol Biogeogr.* 19(3):332–342.
- Zou Y-P, Hou X-H, Wu Q, Chen J-F, Li Z-W, Han T-S, Niu X-M, Yang L, Xu Y-C, Zhang J, et al. 2017. Adaptation of *Arabidopsis thaliana* to the Yangtze River basin. *Genome Biol.* 18(1):239.